Metabolic Engineering 13 (2011) 508–517

Contents lists available at ScienceDirect

Metabolic Engineering

journal homepage: www.elsevier.com/locate/ymben

Kinetic modelling reveals current limitations in the production of ethanol from xylose by recombinant *Saccharomyces cerevisiae*

Nádia Skorupa Parachin, Basti Bergdahl, Ed W.J. van Niel, Marie F. Gorwa-Grauslund *

Department of Applied Microbiology, Center for Chemistry and Chemical Engineering, Lund University, P.O. Box 124, SE-221 00 Lund, Sweden

ARTICLE INFO

Article history:
Received 1 December 2010
Received in revised form
16 May 2011
Accepted 19 May 2011
Available online 27 May 2011

Keywords:
Saccharomyces cerevisiae
Xylose
Ethanol
Kinetic model
Xylitol
Xylulokinase

ABSTRACT

Saccharomyces cerevisiae lacks the ability to ferment the pentose sugar xylose that is the second most abundant sugar in nature. Therefore two different xylose catabolic pathways have been heterologously expressed in *S. cerevisiae*. Whereas the xylose reductase (XR)-xylitol dehydrogenase (XDH) pathway leads to the production of the by-product xylitol, the xylose isomerase (XI) pathway results in significantly lower xylose consumption. In this study, kinetic models including the reactions ranging from xylose transport into the cell to the phosphorylation of xylulose to xylulose 5-P were constructed. They were used as prediction tools for the identification of putative targets for the improvement of xylose utilization in *S. cerevisiae* strains engineered for higher level of the non-oxidative pentose phosphate pathway (PPP) enzymes, higher xylulokinase and inactivated *GRE3* gene encoding an endogenous NADPH-dependent aldose reductase. For both pathways, the *in silico* analyses identified a need for even higher xylulokinase (XK) activity. In a XR-XDH strain expressing an integrated copy of the *Escherichia coli* XK encoding gene *xylB* about a six-fold reduction of xylitol formation was confirmed under anaerobic conditions. Similarly overexpression of the *xylB* gene in a XI strain increased the aerobic growth rate on xylose by 21%. In contrast to the *in silico* predictions, the aerobic growth also increased 24% when the xylose transporter gene *GXF1* from *Candida intermedia* was overexpressed together with *xylB* in the XI strain. Under anaerobic conditions, the XI strains overexpressing *xylB* gene and the combination of *xylB* and *GFX1* genes consumed 27% and 37% more xylose than the control strain.

1. Introduction

Xylose is the second most abundant sugar in nature and its utilization by baker's yeast *Saccharomyces cerevisiae* would significantly decrease the production cost of bioethanol from a wide range of lignocellulosic biomass (Rudolf et al., 2009). Therefore two different pathways have been introduced in *S. cerevisiae* (Fig. 1) enabling xylose utilization (Eliasson et al., 2000; Karhumaa et al., 2007; Kuyper et al., 2003). The reductive/oxidative pathway, consisting of xylose reductase (XR), EC1.1.1.21 and xylitol dehydrogenase (XDH), EC1.1.1.175, usually from *Pichia stipitis*, converts xylose to xylulose with xylitol as intermediate. The other pathway is an isomerization most frequently encountered in bacteria but also present in some fungi. In this case, xylose is directly converted to xylulose by xylose isomerase (XI), EC5.3.1.5. In both pathways, xylulose enters the pentose phosphate pathway (PPP) by its conversion to xylulose-5-phosphate catalyzed by the enzyme xylulokinase (XK) EC2.7.1.17. In both pathways, the overexpression of the non-oxidative part of PPP encoding genes (Karhumaa et al., 2005; Kuyper et al., 2005) and deletion of *GRE3* gene encoding an endogenous NADPH-dependent aldose reductase (Träff et al., 2001) have been shown to benefit xylose fermentation.

A recent study has compared the two xylose catabolic pathways in an isogenic *GRE3* deleted strain overexpressing the genes encoding the non-oxidative PPP enzymes and the endogenous XK (Karhumaa et al., 2007). Heterologous expression of XR and XDH encoding genes from *P. stipitis* gave higher specific ethanol productivity as a result of a significantly higher xylose consumption rate. However xylitol formation arising from the cofactor imbalance between XR and XDH was higher for XR-XDH strain than for the strain expressing the XI encoding gene, where ethanol yields close to theoretical were achieved (Karhumaa et al., 2007). Enzyme engineering of both XR and XDH have aimed to neutralize the redox balance between these two enzymes (Bengtsson et al., 2009; Jeppsson et al., 2006; Matsushika et al., 2008; Petschacher and Nidetzky, 2008; Runquist et al., 2010a; Watanabe et al., 2007; Zeng et al., 2009). Although this has reduced xylitol formation significantly, still about 15% of the consumed xylose is secreted as xylitol

* Corresponding author.
E-mail address: Marie-Francoise.Gorwa@tmb.lth.se (M.F. Gorwa-Grauslund).

1096-7176/$ - see front matter © 2011 Elsevier Inc. All rights reserved.
doi:10.1016/j.ymben.2011.05.005

Nomenclature

α	relative mobility between bound and unbound transport (dimensionless)
A_{cell}	specific surface area of the cell (m^2/g CDW)
C_x	cell concentration (g/L)
r_x	rate of cell death (/h)
P_x	mass density of cells (g CDW/(L cell volume))
P_{xyt}	permeability coefficient for xylitol (m/s)
CDW	cell dry weight (g/L)
rt_{xyt}	xylitol diffusion rate (mmol/g CDW/h)
$V_{max}^{Xi,f}$	xylose isomerase forward (mM/h)
$V_{max}^{Xi,r}$	xylose isomerase reverse (mM/h)
K_i	inhibition constant (mM)
XDH	xylose dehydrogenase (dimensionless)
V_{max}	maximum velocity (mM/h)
K_m	Michaelis constant (mM)
[XR]	concentration of xylose reductase (U/mg)
XYL_e	xylose extracellular (g/L)
XYL	xylose intracellular (mM)
XYLU	xylulose (mM)
XYT	xylitol intracellular (mM)
XYT_e	xylitol extracellular (g/L)

by the most successful mutants (Bengtsson et al., 2009; Petschacher and Nidetzky, 2008; Runquist et al., 2010a). In the XI pathway, heterologous overexpression of XI encoding genes in *S. cerevisiae* has proved to be a challenging task marked by low enzyme activity in yeast (Amore and Hollenberg, 1989; Gárdonyi and Hahn-Hägerdal, 2003; Moes et al., 1996; Sarthy et al., 1987; Walfridsson et al., 1996). Among the numerous investigated XI encoding genes, only three have been so far reported to result in aerobic (Brat et al., 2009; Kuyper et al., 2003; Madhavan et al., 2008) or anaerobic (Kuyper et al., 2004) growth on xylose.

Mainly confirmatory results have been obtained when metabolic flux analysis (MFA) has been used to describe pentose conversion into metabolic intermediates and to predict fluxes towards product formation (Bengtsson et al., 2009; Pitkanen et al., 2003; Sonderegger et al., 2004; Wahlbom et al., 2001; Wisselink et al., 2010). In the present study kinetics for the enzymes of the two xylose catabolic pathways were used to identify targets for increasing the flux of either pathway at the enzyme level. First kinetic parameters were estimated by fitting the two kinetic models to literature data for xylose fermentation by XR-XDH and XI recombinant *gre3*-deleted strains overexpressing the non-oxidative PPP and the endogenous XK genes. Then the XR-XDH and XI models were used to *in silico* simulate minimal xylitol formation and maximum xylose uptake, respectively. Finally genetically modified strains were constructed in the same strain background and used to *in vivo* validate the *in silico* predictions.

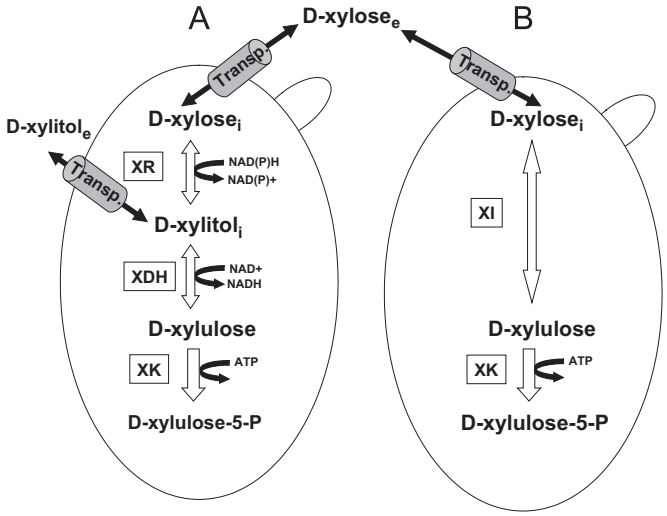

Fig. 1. Initial steps of xylose utilization via reductive/oxidative (A) or isomerization pathway (B). Xylose$_e$ and xylose$_i$ are extracellular and intracellular xylose, respectively.

2. Material and methods

2.1. Kinetic model

Two kinetic models were constructed in Matlab version R2006b within the Systems Biology Toolbox[2] (Schmidt and Jirstrand, 2006). Experimental data were obtained from previously described fermentations for parameter estimation (Karhumaa et al., 2007). Briefly 5 g/L cell dry weight (CDW) of *S. cerevisiae* recombinant *gre3*-deleted strains that have the endogenous XK encoding gene and non-oxidative PPP genes overexpressed, thereby only differing in their initial xylose catabolic pathway (XI or XR/XDH) were utilized in anaerobic batch fermentations containing 50 g/L xylose (Karhumaa et al., 2007).

Kinetic parameters of XR (Rizzi et al., 1988), XDH (Eliasson et al., 2001) and XI (Brat et al., 2009; Vanbastelaere et al., 1991) were taken from studies using pure enzymes. In addition, kinetic parameters for transport was previously determined (Runquist et al., 2010b) in the exact same background as the strains used for the construction of the model and the strains later constructed for its validation. Finally cell parameters including specific cell surface area (A_{cell}) (Tochampa et al., 2005), cell mass density (p_X) (Tochampa et al., 2005) and permeability coefficient for xylitol (P_{xyt}) (Tochampa et al., 2005) were taken from *Candida mogii* and validated by fitting the models to fermentation data (Karhumaa et al., 2007) (Supplementary Fig. 1A and B).

The first model had XR/XDH and the second had XI as first step in xylose conversion. Table 1 summarizes biochemical reactions and enzymes considered in this study. Based on these reactions a set of ordinary differential equations was used to describe the time dependence of metabolite concentrations. For the strain with the XR/XDH pathway the following equations were used:

$$\frac{d(XYL_e)}{dt} = (-V_{trsp,in} + V_{trsp,out})C_x \quad (1)$$

$$\frac{d(XYL)}{dt} = (V_{trsp,in} - V_{trsp,out})P_x - V_{XR} \quad (2)$$

Table 1
Biochemical reactions used in the construction of the kinetic models. (↔) reversible; (→) irreversible. e = extracellular.

Reaction	Name	Enzymes	Reactant	Product
1 (↔)	Transport	Transporter	Xylose$_e$	Xylose
2 (↔)	XR	Xylose reductase	Xylose	Xylitol
3 (↔)	XDH	Xylitol dehydrogenase	Xylitol	Xylulose
4 (→)	XK	Xylulokinase	Xylulose	Xylulose-5-P
5 (↔)	XYT diff	Transporter	Xylitol	Xylitol$_e$
6 (↔)	XI	Xylose isomerase	Xylose	Xylulose

$$\frac{d(XYT)}{dt} = V_{XR} - V_{XDH} - P_x rt_{xyt} \quad (3)$$

$$\frac{d(XYT_e)}{dt} = rt_{xyt} C_x \quad (4)$$

$$\frac{d(XYLU)}{dt} = V_{XDH} - V_{XK} \quad (5)$$

$$\frac{dC_x}{dt} = -C_x r_x \quad (6)$$

For XI strain the equations were:

$$\frac{d(XYL_e)}{dt} = (-V_{trsp,in} + V_{trsp,out}) C_x \quad (7)$$

$$\frac{d(XYL)}{dt} = (V_{trsp,in} - V_{trsp,out}) P_x - V_{XI} \quad (8)$$

$$\frac{d(XYLU)}{dt} = V_{XI} - V_{XK} \quad (9)$$

$$\frac{dC_x}{dt} = -C_x r_x \quad (10)$$

All enzymatic rate expressions with their respective kinetic parameters are listed in supplementary Table 1. In both models a differential equation that defines cell inactivation over time was added (Eq. (6) for the XR/XDH model and Eq (10) for the XI model). All maximum velocities (V_{max}) were calculated based on the values of enzyme activities in crude extracts. The activities (mmol/h) were multiplied by the total protein content per cell dry weight (CDW) according to Teusink et al. (2000) and by the specific cell volume as previously described (de Koning and van Dam, 1992). For the model of the XR/XDH pathway a reaction for xylitol excretion was included as previously described (Tochampa et al., 2005) and it was validated by fitting xylose consumption and xylitol production to fermentation data from a previously published study using a XR/XDH strain carrying *gre3* deletion and overexpression of the non-oxidative PPP and XK genes (Karhumaa et al., 2007). The simulation correlated with experimental data with an $R^2 = 0.962$ (Supplementary Fig. 1A). Some assumptions were also made to simplify the kinetic analysis:

(I) Initial biomass was 5 g/L (CDW) and it was considered constant since no changes in OD was observed during the experiments.

(II) Intracellular concentrations of ATP and relevant co-factors were assumed to be constant with the following values measured elsewhere under usual fermentation conditions (Hynne et al., 2001; Satrustegui et al., 1983): ATP = 0.534 mM, NADPH = 0.487 mM, $NADP^+$ = 0.0657 mM, NADH = 0.553 mM, NAD^+ = 2.767 mM.

(III) Xylitol production resulting from endogenous yeast reductases (Träff et al., 2002) was disregarded in both models.

(IV) In the XR/XDH model, the xylose reductase reaction (XR) was considered only NADPH dependent even though it also utilizes NADH as cofactor (Eliasson et al., 2001). This is due to the fact that the affinity for NADH is much lower than the affinity for NADPH (Bengtsson et al., 2009) so when both co-factors are present the contribution to the total rate of xylitol formation by the NADH-dependent reaction can be neglected. By assuming that the XR cannot use NADH the complexity of the rate equation could be significantly reduced with only a small underestimation of the reaction rate.

(V) The phosphorylation of xylulose into xylulose-5P coupled with ATP hydrolysis was considered unidirectional and the rate of conversion was assumed to be dependent on the concentrations of xylulose and ATP only.

(VI) In the XI model, the rate equation for the XI reaction was described as a reversible Michaelis–Menten reaction with the following relationship between the forward and reverse reaction velocities: $V_{max}^{XI,r} = 1.3 \times V_{max}^{XI,f}$ as formerly observed (Vanbastelaere et al., 1991). Consequently, an increase in the V_{max} of the forward reaction would give an increase in the maximum velocity of the reverse reaction.

Evaluation of the effect of changing the level of individual enzymes was done by manually increasing or decreasing the activity values (V_{max}) by an order of magnitude of 10, *i.e.* an average value of what can be achieved by gene overexpression/deletion.

2.2. Plasmids, strains and cultivation conditions

Plasmids and strains used in this study are listed in Table 2. *Escherichia coli* DH5α (Life Technologies, Rockville, MD, USA) was used for subcloning prior to yeast transformation. All strains were stored as 20% glycerol stocks in liquid media at −80 °C.

S. cerevisiae strains were plated on YNB-media plates (6.7 g/L YNB w/o amino acids, Difco, Becton, Dickinson and Company,

Table 2
Plasmids and strains used in this study.

Plasmid/strain	Relevant genotype	Reference
Plasmids		
p426TEF	*URA3*, *TEF*p-*CYC1*t	Mumberg et al. (1995)
YIplac128	*LEU2*	Gietz and Sugino (1988)
YIplac204	*TRP1*	Gietz and Sugino (1988)
YIpOB9	*URA3*, *TDH3*p-*XYL1*(K270R)-*CYC1*t, *PGK1*p-*XYL2*-*PGK1*t	Bengtsson (2008)
p426TEF-XiPiromyces	p426, *URA3*, *TEF*p-*xylA*-*CYC1*t	This study
YIpDR1	YIplac128, *TDH3*p-*GXF1*-*CYC1*t, *LEU2*	Runquist et al. (2009)
YIpXKEC	YIplac128, *TDH3*p-*xylB*-*CYC1*t, *LEU2*	This study
YIpGXF1	YIplac204, *TDH3*p- *GXF1*-*CYC1*t, *TRP1*	
Strains		
TMB3042	CEN.PK 2-1C Δ*gre3*, *his3*::*PGK1*p-*XKS1*-*PGK1*t, *TAL1*::*PGK1*p-*TAL1*-*PGK1*t, *TKL1*::*PGK1*p-*TKL1*-*PGK1*t, *RKI1*::*PGK1*p-*RKI1*-*PGK1*t, *RPE1*::*PGK1*p-*RPE1*-*PGK1*t, *trp1, leu2, ura3*.	Karhumaa et al. (2005)
TMB3367	TMB 3042, *trp1*::YIplac204, *leu2*::YIplac128, *ura3*::YIpOB9	This study
TMB3368	TMB 3042, *trp1*::YIplac204, *leu2*::YIpXKEC, *ura3*::YIpOB9	This study
TMB3359	TMB3042, *trp1*::YIplac204, *leu2*::YIplac128, *ura3*:: p426TEFXi	This study
TMB3360	TMB 3042, *trp1*::YIplac204, *leu2*::YIpDR1, *ura3*:: p426TEFXi	This study
TMB3361	TMB 3042, *trp1*::YIplac204, *leu2*::YIpXKEC, *ura3*::p426TEFXi	This study
TMB3362	TMB 3042, *trp1*::YIpGXF1, *leu2*::YIpXKEC, *ura3*::p426TEFXi	This study

Sparks, MD, USA) supplemented with 20 g/L glucose and 20 g/L agar. The amino acids L-tryptophan, L-leucine as well as uracil were added to a final concentration of 76 mg/L when needed. *S. cerevisiae* strains were pre-grown in 1 L Erlenmeyer flasks containing 100 mL YNB-medium (6.7 g/L YNB w/o amino acids, 20 g/L glucose) at 180 rpm and 30 °C for approximately 12 h. Cells were subsequently inoculated at $OD_{620\ nm}=0.2$ in 100 mL YNB-medium supplemented with 50 g/L xylose in 1-L Erlenmeyer flasks and grown at 180 rpm and 30 °C. In anaerobic fermentations 400 mg/L Tween 80 and 10 mg/L ergosterol were added to twice concentrated YNB.

2.3. Strain construction

Standard techniques for DNA manipulation were used as previously described (Sambrook et al., 1989). Restriction and ligation enzymes were purchased from Fermentas (St. Leon-Rot, Germany). Primers were purchased from Eurofins MWG Operon (Ebersberg, Germany). DNA extraction from agarose gels and purification of PCR products were performed with the QIAquick extraction kit (Qiagen, Hilder, Germany). Plasmid DNA was prepared with the Biorad miniprep kit (Hercules, CA, USA). Sequencing was performed at Eurofins MWG Operon (Ebersberg, Germany). Yeast transformation was performed as previously described (Gietz et al., 1995).

The XK encoding gene *xylB* from *E. coli* was amplified by PCR using genomic DNA from strain DH5α (Life Technologies, Rockville, MD, USA), primer forward: 5′ TCC*ACTAGT*ATGTATATCGGGATAGATCTTGGCACC 3′ and reverse: 5′ CCG*GTCGAC*TTACGCCATTA ATGGCAGAAGTTGCTG 3′. Restriction sites for *Spe*I and *Sal*I are underlined in primers forward and reverse, respectively. Plasmid YIpDR1 (Runquist et al., 2009) (Table 2) was restricted with the same enzymes used for the PCR product restriction. The fragment of 5.2 kb corresponding to the vector without *GXF1* was purified from agarose gel and used as backbone for the ligation with the restricted PCR-amplified XK gene. After insert confirmation, by sequencing, plasmid YIpXKEC (Table 2) was linearized with *Bbs*I, which cuts in *LEU2* gene prior to plasmid integration.

For construction of YIpGXF1, plasmid YIpDR1 was restricted with *Pst*I and *BamH*I. The fragment of approximately 2.6 kb containing the *TDH3* promoter, the glucose/xylose facilitator *GFX1* gene from *Candida intermedia* and the *CYC1* terminator (Runquist et al., 2009) was ligated into YIplac204 previously restricted with the same enzymes. The resulting plasmid YIpGXF1 (Table 2) was linearized with *Eco*RV, which cuts inside *TRP1* gene, prior to integration into yeast.

XI gene from *Piromyces sp.* was amplified by PCR utilizing plasmid YeplacHXT-XI as template (Karhumaa et al., 2005), primer forward: 5′GGA*GGATCC*ATGGCTAAGGAATATTTTCCACAAATTC 3′ and reverse: 5′ TTG*GAATTC*TTACTGATACATTGCAACAATAGCTTCG 3′. Restriction sites for *BamH*I and *Eco*RI are underlined in primers forward and reverse, respectively. Plasmid p426TEF (Mumberg et al., 1995) and the PCR product were restricted with *BamH*I and *Eco*RI and then ligated. Clones with insert were sequenced prior to yeast transformation.

Construction of recombinant *S. cerevisiae* strains for model validation were done using strain TMB3042 that has the same background as the strain utilized for the model construction, *i.e.* overexpressed genes encoding the non-oxidative PPP enzymes and XK and deleted *GRE3* gene (Table 2). Construction of recombinant strain TMB3368 containing XR/XDH pathway and an extra copy of XK was done by sequential integration of linearized YIplac204 (Gietz and Sugino, 1988), YIpXKEC and plasmid YIpOB09 carrying the XR and XDH genes (Bettiga et al., 2009) . The control strain for the XR/XDH pathway, TMB3367, was constructed by integration of linearized YIplac128 (Gietz and Sugino, 1988) instead of YIpXKEC.

The control strain carrying the XI pathway, TMB3359, was obtained by sequential integration of linearized YIplac204 (Gietz and Sugino, 1988), linearized YIpXKEC and the multicopy plasmid p426TEFXI. For the strains carrying the XI pathway in combination with only transport, or an extra copy of XK, TMB3042 was sequentially transformed with YIplac204, YIpDR1 (TMB3360) or YIpXKEC (TMB3361). Finally both strains were transformed with the multicopy plasmid p426TEFXi. Strain TMB3362, carrying both transport and an extra copy of XK was constructed by sequential yeast transformation with YIpGXF1, YIpXKEC and p426TEFXi.

2.4. Enzyme activities

For enzymatic activity measurements, strains were cultivated in YNB medium with 20 g/L glucose and harvested at stationary phase. Cells were washed twice with distilled water and treated with yeast protein extract solution Y-PER (Pierce, Rockford, IL, USA). XI activity was determined using sorbitol dehydrogenase as previously described (Kuyper et al., 2003) at 30 °C. XK activity was measured by coupling ADP production to NADH oxidation via pyruvate kinase as earlier described (Di Luccio et al., 2007). Variations of XK activity, when compared to previous studies (Karhumaa et al., 2005), may be attributed to the fact that the XK assay is usually not performed at V_{max}, due to the cost of pure xylulose. As a consequence, large differences in protein concentrations will impact the final result. Assays were performed using a spectrophotometer U-2000 (Hitachi, Tokyo, Japan). Protein concentration of cell extracts was determined with Coomassie protein assay reagent (Pierce, Rockford, USA) according to the manufacturer's instructions. Enzyme assays were performed in three biological replicates.

2.5. Anaerobic xylose fermentation

Pre-cultures were grown aerobically in 100 mL of YNB medium with 20 g/L glucose. Cells were harvested in late exponential phase and washed twice in sterile water. Anaerobic fermentation was performed in 50 mL bottles containing 48 mL YNB medium with 50 g/L xylose, 0.01 g/L ergosterol, 0.4 g/L Tween 80, 5 g/L CDW and a layer of sterile mineral oil to reduce oxygen transfer. Bottles were supplied with rubbers stoppers containing cannulae for gas outlet and sampling. The temperature was 30 °C and magnetic stirrers provided agitation. Substrate consumption and product formation were monitored by sampling during 100 h. Experiments were performed in biological triplicates.

2.6. Aerobic growth on xylose

Pre-cultures were grown in YNB medium with 20 g/L glucose and harvested in late exponential phase. Cells were washed twice in sterile water and inoculated in YNB medium containing 50 g/L xylose to a starting OD_{620} of 0.2. Specific aerobic growth rates were determined in 50 mL culture in 500 mL baffled shake flasks at 30 °C and 200 rpm (Gallenkamp INR200, Leicester, UK). Growth rates were determined in triplicate.

2.7. Analysis of fermentation products

Substrate and product concentrations were determined by high-performance liquid chromatography (HPLC; waters, Milford, MA, USA) with Aminex HPX-87 H ion exchange column (Bio-Rad, Hercules, CA, USA) using 5 mM H_2SO_4 as mobile phase and refractive index detection (RID-6A, Shimadzu, Kyoto, Japan). The temperature and flow rate were 45 °C and 0.6 mL/min, respectively.

In addition to ethanol, only xylitol, glycerol and acetate were detected as products. Dry weight was determined in triplicates. Nitrocellulose filters with 0.45 μm pore size were dried in a microwave oven for 3 min and left to cool down in a dessicator. Filters were weighed prior to filtering a known volume of cell culture. Dry weight was the difference between the dried filter with and without cells.

3. Results

3.1. Kinetic model

Kinetic models were constructed for the two xylose catabolic pathways. The models included the steps from xylose transport to the phosphorylation of xylulose (Fig. 1, Table 1 and supplementary Table 1) thus reflecting the only metabolic differences between the otherwise isogenic strains (Karhumaa et al., 2007). The models for the XR-XDH and XI pathway were constructed using available cell parameters including specific cell surface area (A_{cell}) (Tochampa et al., 2005), cell mass density (p_X) (Tochampa et al., 2005), permeability coefficient for xylitol (P_{xyt}) (Tochampa et al., 2005) and maximum velocity (V_{max}) for xylose transport (Runquist et al., 2010b). Those were validated concomitant with calculated V_{max} for XR, XDH, XI and XK by fitting the models to fermentation data (Karhumaa et al., 2007) (Supplementary Fig. 1A and B).The calculated values as well as the fitted ones for V_{max} of transport, XR, XDH, XK and XI are listed in the supplementary Table 1.

The XR/XDH model was used to *in silico* simulate minimal xylitol formation with 10-fold changes of individual V_{max} values, which were assumed to correspond to an equal change of protein level (Fig. 2A). The maximum velocity of XDH (V_{max}^{XDH}) did not affect xylitol formation in the range of activities investigated. In contrast xylitol formation was reduced both when the maximum velocity of the transporter (V_{max}^{trsp}) and the maximum velocity of XR (V_{max}^{XR}) were decreased (Fig. 2A), but this also reduced the overall xylose consumption (Fig. 2B). The most significant effect was observed when changing the maximum velocity of XK (V_{max}^{XK}): xylitol production, decreased by 90% when V_{max}^{XK} was increased 10 fold (Fig. 2A), without affecting the total xylose consumption (Fig. 2B).

When using the XI model to simulate how V_{max} of xylose transport and XI, respectively, influenced the total xylose consumption, it was found that neither reaction had a significant effect on xylose consumption (Fig. 2C). In fact, V_{max}^{XI} only affected the total xylose consumption when it decreased below 20% of the fitted value (data not shown). However, similar to the XR-XDH model the largest increase of the total xylose consumption, 63%, was observed when the maximum activity of *XK* (V_{max}^{XK}) was increased 10 fold.

3.2. "in vivo" validation of the XR-XDH model

The predictions of the *in silico* simulations were validated by constructing a number of recombinant *S. cerevisiae* strains having exactly the same background (*gre3* deletion, overexpressed non-oxidative PPP genes and overexpressed XK gene) as the ones utilized for *in silico* simulations (Karhumaa et al., 2007). The only difference concerned XR that carried the K270R mutation resulting in increased affinity for NADH (Bengtsson et al., 2009). Thus the control strain, TMB3367 had overexpressed endogenous XK encoding gene, non-oxidative PPP genes and mutated XR(K270R) in addition to deletion of *GRE3* gene. TMB3368 had exactly the same background than TMB3367 but with an additional copy of a XK encoding gene integrated on the genome (Table 2). The *xylB* gene encoding *E. coli* XK was chosen for the integration because the reported turnover number (k_{cat}) for *S. cerevisiae* XK is only 0.64/s (Richard et al., 2000), whereas that of *E. coli* is 255/s (Di Luccio et al., 2007) despite similar K_m values for both xylulose and ATP. In addition changing the source of XK encoding gene have been shown beneficial in *E. coli* recombinant strains growing on

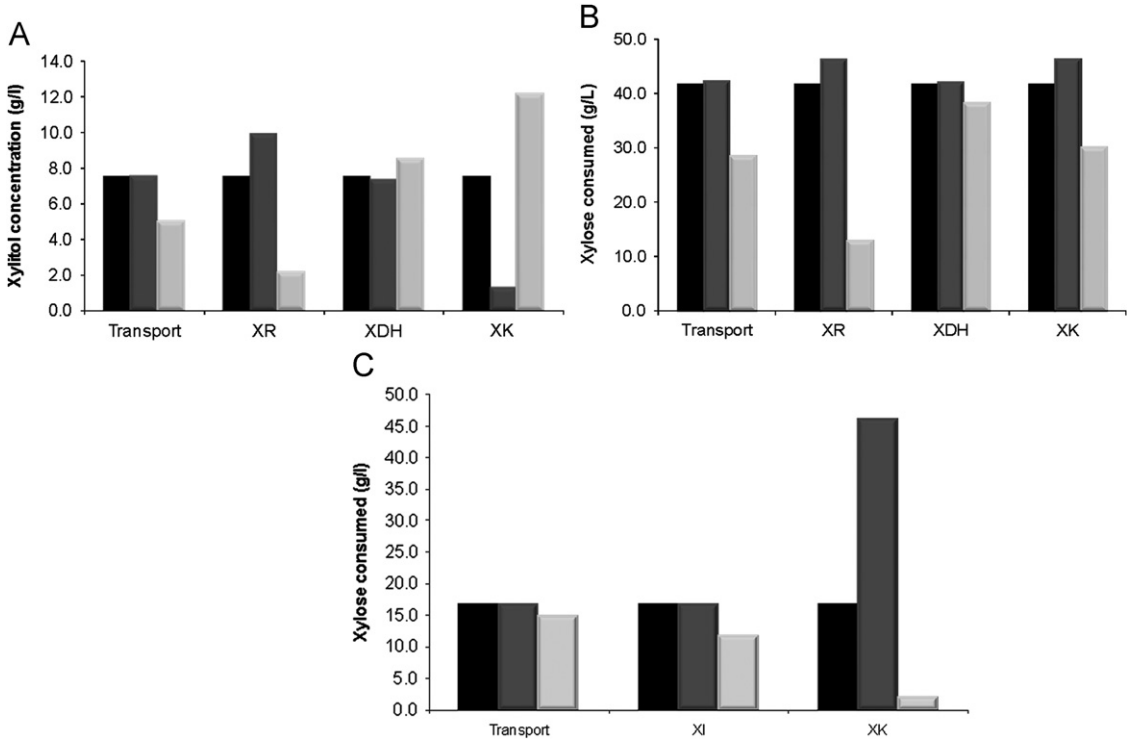

Fig. 2. *In silico* evaluation of individual V_{max} on xylitol formation (A) and total xylose consumption (B) in the XR/XDH kinetic model and total xylose consumption in the XI model (C). Black bars represent values given by the kinetic model; Grey and white bars represent tenfold increased and decreased enzyme activity, respectively.

xylose (Akinterinwa and Cirino, 2009). A doubling of the XK activity (Supplementary Table 2) confirmed the correct expression of *xylB* in *S. cerevisiae*.

The influence of overexpressing *E. coli* XK encoding gene was assessed by aerobic growth and by anaerobic batch fermentation (Fig. 3, Table 3). The aerobic growth rate of the strain overexpressing *xylB* increased 35%. Under anaerobic conditions *xylB* overexpression reduced the xylose consumption rate slightly, resulting in 14% less xylose being consumed at the end of the fermentation than for the control strain, TMB3367 (Fig. 3A). But at the end of the fermentation the final ethanol concentration for the two strains was similar (Fig. 3B), which corresponded to an increased ethanol yield by about 7% for the XK overexpressing strain when calculated on consumed xylose. The major difference between the strains was xylitol and glycerol formation. Overexpressing the *E. coli* XK gene led to a 6-fold reduction of xylitol formation corresponding to about 1% of total xylose consumed (Fig. 3C). The reduced xylitol formation translated into increased glycerol formation by strain TMB3368, two times more than what was produced by the control strain, TMB3367 (Fig. 3D and Table 3).

3.3. *In vivo* validation of the XI model

Similar to the XR-XDH model the XI model identified the XK reaction as limiting rather than xylose transport and XI. However, for the *in vivo* validation of the XI model we investigated both the XK reaction and the xylose transport in order to test the robustness of the model. It was not technically possible to *in vivo* corroborate that higher XI level does not positively affect xylose utilization because the XI encoding gene was already cloned into a multicopy plasmid and under the regulation of a strong promoter.

Four recombinant strains, all harbouring the *Piromyces sp*. XI gene overexpressed in the same strain background as the one used for the validation of the XR-XDH model, were constructed: (i) the control strain TMB3359, (ii) strain TMB3360 where the xylose transport capacity was increased by overexpressing the heterologous transporter gene *GFX1* from *C. intermedia* (Runquist

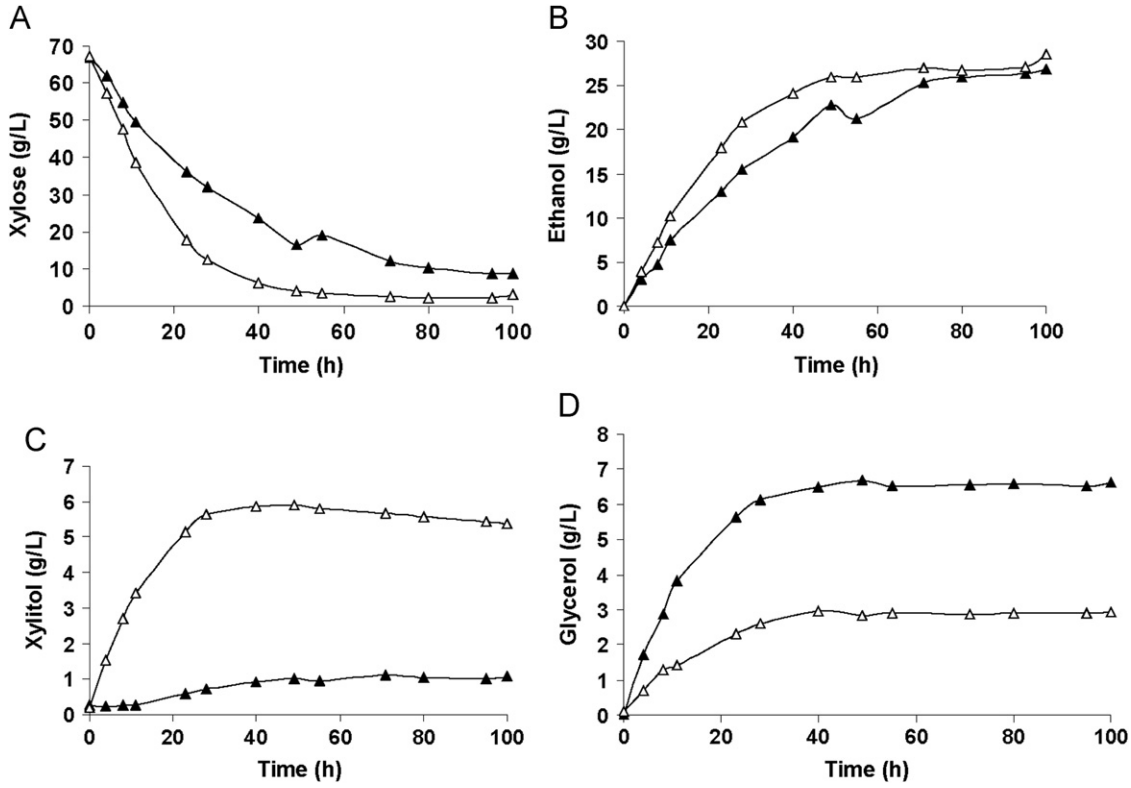

Fig. 3. Anaerobic xylose batch fermentation with the control strain TMB3367 (△) and strain TMB3368 overexpressing *E. coli* XK encoding gene *xylB* (▲) showing xylose consumption (A) (g L h^{-1}) as well as ethanol (B), xylitol (C) and glycerol (D) formation (g L^{-1}). Experiments were performed in triplicates, with less than 10% variation between replicates.

Table 3
Aerobic maximum specific growth rate on xylose (h^{-1}). Anaerobic substrate consumption (g/L) and product yield (g product/g total consumed xylose) in batch fermentation with YNB medium containing 60 g/L xylose. Aerobic growth rates were determined from independent triplicates ($p < 0.05$).

Strain	Main characteristic	Aerobic	Anaerobic			
		μ_{max} (h^{-1})	Xylose consumed	Xylitol yield	Ethanol yield	Glycerol yield
TMB3367	XR/XDH-CTRL	0.13 ± 0.02	64.4 ± 0.6	0.09 ± 0.01	0.43 ± 0.01	0.075 ± 0.02
TMB3368	XR/XDH+XK *E. coli*	0.20 ± 0.01	56.7 ± 2.1	0.01 ± 0.01	0.46 ± 0.01	0.125 ± 0.006
TMB3359	Xi- CTRL	0.070 ± 0.007	17.5 ± 1.0	0.06 ± 0.01	0.42 ± 0.04	0.045 ± 0.012
TMB3360	Xi+Transport	0.081 ± 0.003	18.7 ± 0.5	0.06 ± 0.01	0.40 ± 0.07	0.086 ± 0.008
TMB3361	Xi+XK *E. coli*	0.089 ± 0.002	24.1 ± 0.8	0.05 ± 0.01	0.41 ± 0.05	0.044 ± 0.016
TMB3362	Xi+transport+XK *E. coli*	0.093 ± 0.008	27.9 ± 0.7	0.03 ± 0.01	0.43 ± 0.07	0.023 ± 0.005

et al., 2009), (iii) strain TMB3361, where the XK activity increased by overexpression of the *E. coli* XK encoding gene and (iv) strain TMB3362 combining high transport capacity and high XK activity (Table 2). We confirmed that all four strains displayed similar levels of XI activity, whereas the XK activity was increased in strains TMB3361 and TMB3362 (Supplementary Table 2).

The *in silico* predictions of the XI model were verified *in vivo* by aerobic growth (Fig. 4) and anaerobic fermentation (Fig. 5) on xylose. The aerobic growth rate increased for the two strains with increased XK activity (Fig. 4). The strain overexpressing the heterologous xylose transporter gene *GXF1*, TMB3360, had a longer lag phase but eventually had a growth rate similar to that of the control strain, TMB3359. The growth rate of the strain overexpressing the *E. coli* XK gene increased 21% (p_{value}=0.041) whereas the strain harbouring both the heterologous transporter and the *E. coli* XK gene, TMB3362, had the shortest lag phase and a 24% (p_{value}=0.008) higher growth rate than the control strain (Table 3). The final OD of strain TMB3361, harbouring the integrated copy of the *E. coli* XK gene, was the same as for the control strain TMB3359. However, for strains TMB3360 and TMB3362, with increased transport capacity and the combination of increased transport and XK activity, respectively, the final OD was about 20% higher than that of the control strain.

Anaerobic batch fermentation with the recombinant XI-based *S. cerevisiae* strains confirmed that overexpression of the *GXF1* transporter gene *per se* did neither increase xylose consumption nor ethanol formation (Table 3, Fig. 5). In contrast, the total (100 h) xylose consumption increased by 27% and 37% when overexpressing the *E. coli* XK gene, alone or together with the overexpression of the *GXF1* transporter, respectively. The ethanol yield was about the same for the four XI-strains (Table 3). However, since strains TMB3361 (higher XK activity) and TMB3362 (higher XK and transport capacity) consumed more xylose these two strains produced 1.3 and 2 times more ethanol, respectively (Fig. 5).

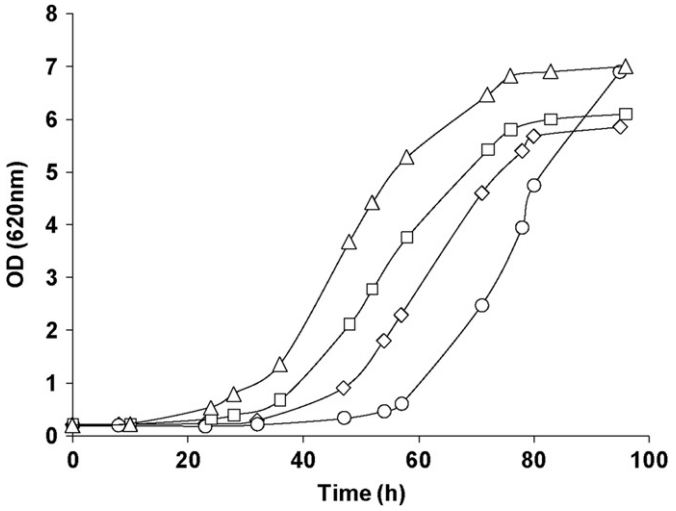

Fig. 4. Aerobic growth of XI strains in mineral media containing 50 g/L xylose. Control strain TMB3359 (⋄), strain TMB3360 overexpressing *GXF1* transporter gene from *C. intermedia* (○), strain TMB3361 overexpressing *E. coli* XK gene *xylB* (□) and strain TMB3362 overexpressing *xylB* and *GXF1* genes (△). Experiments were performed in triplicates, with less than 10% variation between triplicates.

4. Discussion

The present study demonstrates, for the first time, how *in silico* simulations can be used to identify rate-controlling reactions in the initial xylose catabolic pathways heterologously expressed in recombinant *S. cerevisiae* strains. Kinetic models were constructed for the initial XR-XDH and XI pathways using literature data (Eliasson et al., 2001; Rizzi et al., 1988; Tochampa et al., 2005; Vanbastelaere et al., 1991) and experimental data from xylose fermentation (Karhumaa et al., 2007). Both models identified the XK activity as a rate-controlling step in the recombinant *S. cerevisiae* strains, which have been engineered for xylose utilization with a combination of various traits (increased level of the non-oxidative PPP enzymes, increased level of the endogenous XK, deletion of *GRE3* gene and more balanced cofactor utilization between XR and XDH or high XI level). The rate controlling function of the XK reaction was experimentally verified in strains expressing the two different initial xylose catabolic pathways.

The endogenous XK activity has previously been demonstrated to limit xylose utilization (Ho et al., 1998). Expression of the *S. cerevisiae* XK gene from an episomal multicopy plasmid confirmed the importance of the XK activity (Johansson et al., 2001). It doubled the ethanol yield and reduced xylitol formation by 70%, however, at the expense of a 50% reduction of the xylose consumption rate (Johansson et al., 2001). Subsequently the expression of different levels of *S. cerevisiae* (Lee et al., 2003) and *P. stipitis* (Jin et al., 2003) XK encoding genes corroborated that the xylose consumption rate was reduced when the XK gene was expressed from an episomal multicopy plasmid, whereas the xylulose consumption rate increased almost six times when the

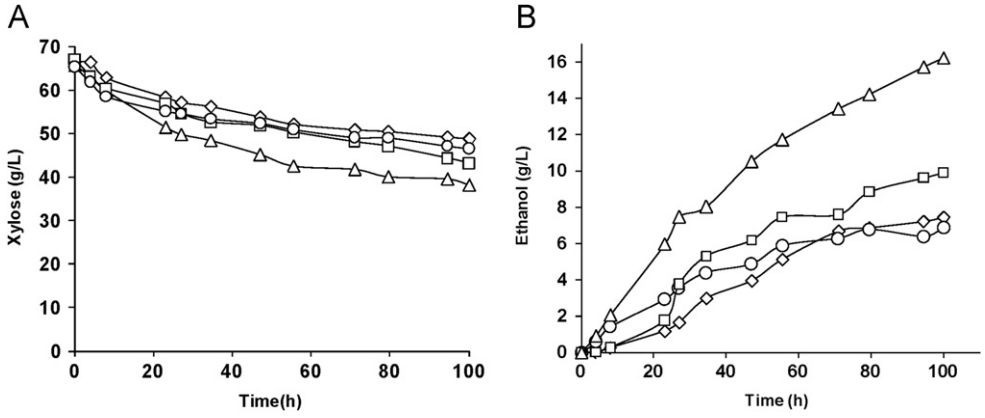

Fig. 5. Anaerobic xylose batch fermentation showing xylose consumption (g L^{-1}) (A) and ethanol formation (g L^{-1}) (B). Control strain TMB3359 (⋄), strain TMB3360 overexpressing *GXF1* transporter gene from *C. intermedia* (○), strain TMB3361 overexpressing *E. coli* XK gene *xylB* (□) and strain TMB3362 overexpressing *xylB* and *GXF1* genes (△). Experiments were performed in triplicates, with less than 10% variation between replicates.

S. cerevisiae XK encoding gene was instead chromosomally integrated (Lee et al., 2003). Moreover high levels of endogenous XK have been shown to reduce growth on high concentrations of xylose (Van Vleet et al., 2008). Therefore an integrated copy of the XK encoding gene has been considered sufficient to establish a xylose catabolic pathway in *S. cerevisiae* (Karhumaa et al., 2005; Kuyper et al., 2004). Nonetheless the present study demonstrates that XK is again limiting in the current generation of strains that combine high non-oxidative PPP activity, deletion of the *GRE3* gene and a more balanced cofactor utilization between XR and XDH or a high XI level. In the XR-XDH strain, the overexpression of *E. coli* XK encoding gene led to a reduction of xylitol yield from 0.09 to 0.01 g/g consumed xylose, which is even less than obtained with XI strains (Table 3) (Brat et al., 2009; Karhumaa et al., 2007; Madhavan et al., 2009, 2008).

When the XK encoding gene was overexpressed in the XI strain the total xylose consumption increased by a factor of 27% and when higher XK was combined with higher transport capacity xylose consumption increased by a factor of 37%. This agrees with the fact that the isomerization reaction thermodynamically favors xylose formation at 30 °C (Tewari et al., 1985) and that xylulose must be continuously converted to xylulose-5-P to maintain xylose consumption. Indeed, XI strains with native levels of XK have been reported both to secrete xylulose (van Maris et al., 2007) and to consume only 10% of the available xylose (Madhavan et al., 2008).

Whereas the kinetic models proved to be valuable for the identification of a rate limiting activity, the models were designed only to cover the initial xylose catabolic pathways. This could, for instance, explain why the significantly lower xylitol yield in the XR-XDH strain was not accompanied by a higher ethanol yield. Instead the glycerol yield increased about two fold. Since fermentation experiments were performed with a high cell density, biomass formation was hardly observed and increased glycerol could not result from a need to regenerate the excess of NADH formed during biosynthesis (Van Dijken and Scheffers, 1986). Instead the combination of increased XK activity and higher flux through the non-oxidative part of the PPP may have increased dihydroxyacetone phosphate (DHAP) formation from glyceraldehyde 3-phosphate (GA3P), which increased the flux towards glycerol formation. Moreover, overexpression of an extra copy of XK encoding gene resulted in a slight reduction of the xylose consumption rate in the XR-XDH strain under anaerobic conditions, which was not predicted by the model. This has been previously observed elsewhere (Jin et al., 2003; Johansson et al., 2001; Lee et al., 2003) and it has been explained due to the increase in the rate of ATP required for sugar phosphorylation (Becker and Boles, 2003; Teusink et al., 1998). The current model did not account for any reduction in xylose consumption because ATP levels were fixed and assumed not to be limiting.

The *in vivo* demonstration of control by the xylose transport reaction illustrated another limitation of the constructed kinetic models. Even after the XK level had been up-regulated, *in silico* simulations were not able to identify any rate control of the xylose transport step in the XI strain (data not shown). Xylose transport capacity has been considered limiting only when the intracellular rate of xylose catabolism has already been improved (Gárdonyi et al., 2003; Runquist et al., 2009), which has been experimentally corroborated for strains with increased XK activity (Madhavan et al., 2008) as well as strains constructed in the current study. Moreover discrepancies between the model and the *in vivo* result may be caused by the conditions under which enzyme activities were measured. Enzyme activities were measured in cell extracts under optimal "*in vitro*" conditions and sometimes with in coupled assays, which do not necessarily reflect the "*in vivo*" conditions (Teusink et al., 2000).

The model also predicted levels of XK, not XI, to be rate-controlling. This supports previous experiments from our group (Karhumaa et al., 2007), where a high and similar level of XI activity as reported by others (Kuyper et al., 2003, 2004) did not results in the same high xylose consumption rate in strains that were, in theory, isogenic. Unfortunately the activity levels of XK and PPP enzymes were not reported, so a comparison could not be made. Xylose fermenting XI strains that are considerably better than those constructed in the current investigation have also been generated through extensive adaptation, but so far the molecular bases for the improvement of these strains are also not available in the public domain (Brat et al., 2009; Kuyper et al., 2005; Madhavan et al., 2009). The present rationally engineered XI strains consumed at most half of the available xylose when both XK and the transport capacity had been increased, suggesting that the XK activity in recombinant strain with XI pathway may have to be further increased. Alternatively there may be one or more rate limiting reactions downstream of XK, since these were not included in the kinetic model. The current models could serve as a base for the construction of more extended kinetic models covering xylose catabolism beyond the initial reactions.

5. Conclusion

In this study, kinetic modelling was successfully used as a designing tool for strains with improved xylose utilization. It resulted in the construction of (i) recombinant XR-XDH strains that produced xylitol concentrations equivalent to that of XI strains and (ii) 59% increase total xylose consumption in recombinant XI strains. In both cases, higher levels of XK were necessary, whereas a combination of increased transport and XK activity proved to be the most advantageous in the XI strain. The constructed models may serve as a base for the construction of more complex models that take into account the steps downstream of XK.

Acknowledgments

Bärbel Hahn–Hägerdal and Elke Lohmeier–Vogel are acknowledged for critically reading the manuscript. This work was financed by the Swedish Research Council (VR) and the Swedish Energy Agency (Energimyndigheten).

Appendix A. Supporting information

Supplementary data associated with this article can be found in the online version at doi:10.1016/j.ymben.2011.05.005.

References

Akinterinwa, O., Cirino, P.C., 2009. Heterologous expression of D-xylulokinase from *Pichia stipitis* enables high levels of xylitol production by engineered *Escherichia coli* growing on xylose. Metab. Eng. 11, 48–55.

Amore, R., Hollenberg, C.P., 1989. Xylose isomerase from *Actinoplanes missouriensis*: primary structure of the gene and the protein. Nucl. Acids Res. 17, 7515.

Becker, J., Boles, E., 2003. A modified *Saccharomyces cerevisiae* strain that consumes L-Arabinose and produces ethanol. Appl. Environ. Microbiol. 69, 4144–4150.

Bengtsson, O., 2008. Genetic traits beneficial for xylose utilization by recombinant *Saccharomyces cerevisiae* Doctoral Thesis. Division of Applied Microbiology. Lund University, Lund.

Bengtsson, O., Hahn-Hägerdal, B., Gorwa-Grauslund, M.F., 2009. Xylose reductase from *Pichia stipitis* with altered coenzyme preference improves ethanolic xylose fermentation by recombinant *Saccharomyces cerevisiae*. Biotechnol. Biofuels 2, 9.

Bettiga, M., Bengtsson, O., Hahn-Hägerdal, B., Gorwa-Grauslund, M.F., 2009. Arabinose and xylose fermentation by recombinant *Saccharomyces cerevisiae* expressing a fungal pentose utilization pathway. Microb. Cell Fact. 8, 40.

Brat, D., Boles, E., Wiedemann, B., 2009. Functional expression of a bacterial xylose isomerase in *Saccharomyces cerevisiae*. Appl. Environ. Microbiol. 75, 2304–2311.

de Koning, W., van Dam, K., 1992. A method for the determination of changes of glycolytic metabolites in yeast on a subsecond time scale using extraction at neutral pH. Anal. Biochem. 204, 118–123.

Di Luccio, E., Petschacher, B., Voegtli, J., Chou, H.T., Stahlberg, H., Nidetzky, B., Wilson, D.K., 2007. Structural and kinetic studies of induced fit in xylulose kinase from *Escherichia coli*. J. Mol. Biol. 365, 783–798.

Eliasson, A., Christensson, C., Wahlbom, C.F., Hahn-Hägerdal, B., 2000. Anaerobic xylose fermentation by recombinant *Saccharomyces cerevisiae* carrying XYL1, XYL2, and XKS1 in mineral medium chemostat cultures. Appl. Environ. Microbiol. 66, 3381–3386.

Eliasson, A., Hofmeyr, J.H.S., Pedler, S., Hahn-Hägerdal, B., 2001. The xylose reductase/xylitol dehydrogenase/xylulokinase ratio affects product formation in recombinant xylose-utilising *Saccharomyces cerevisiae*. Enzyme Microbial Technol. 29, 288–297.

Gárdonyi, M., Hahn-Hägerdal, B., 2003. The *Streptomyces rubiginosus* xylose isomerase is misfolded when expressed in *Saccharomyces cerevisiae*. Enzy. Microbial. Technol. 32, 252–259.

Gárdonyi, M., Jeppsson, M., Líden, G., Gorwa-Grauslund, M.F., Hahn-Hägerdal, B., 2003. Control of xylose consumption by xylose transport in recombinant *Saccharomyces cerevisiae*. Biotechnol. Bioeng. 82, 818–824.

Gietz, R.D., Schiestl, R.H., Willems, A.R., Woods, R.A., 1995. Studies on the transformation of intact yeast cells by the LiAc/SS-DNA/PEG procedure. Yeast 11, 355–360.

Gietz, R.D., Sugino, A., 1988. New yeast-*Escherichia coli* shuttle vectors constructed with in vitro mutagenized yeast genes lacking six-base pair restriction sites. Gene 74, 527–534.

Ho, N.W., Chen, Z., Brainard, A.P., 1998. Genetically engineered *Saccharomyces* yeast capable of effective cofermentation of glucose and xylose. Appl. Environ. Microbiol. 64, 1852–1859.

Hynne, F., Dano, S., Sorensen, P.G., 2001. Full-scale model of glycolysis in *Saccharomyces cerevisiae*. Biophys. Chem. 94, 121–163.

Jeppsson, M., Bengtsson, O., Franke, K., Lee, H., Hahn-Hägerdal, B., Gorwa-Grauslund, M.F., 2006. The expression of a *Pichia stipitis* xylose reductase mutant with higher K(M) for NADPH increases ethanol production from xylose in recombinant *Saccharomyces cerevisiae*. Biotechnol. Bioeng. 93, 665–673.

Jin, Y.S., Ni, H., Laplaza, J.M., Jeffries, T.W., 2003. Optimal growth and ethanol production from xylose by recombinant *Saccharomyces cerevisiae* require moderate D-xylulokinase activity. Appl. Environ. Microbiol. 69, 495–503.

Johansson, B., Christensson, C., Hobley, T., Hahn-Hägerdal, B., 2001. Xylulokinase overexpression in two strains of *Saccharomyces cerevisiae* also expressing xylose reductase and xylitol dehydrogenase and its effect on fermentation of xylose and lignocellulosic hydrolysate. Appl. Environ. Microbiol. 67, 4249–4255.

Karhumaa, K., Garcia-Sanchez, R., Hahn-Hägerdal, B., Gorwa-Grauslund, M.F., 2007. Comparison of the xylose reductase-xylitol dehydrogenase and the xylose isomerase pathways for xylose fermentation by recombinant *Saccharomyces cerevisiae*. Microb. Cell Fact 6, 5.

Karhumaa, K., Hahn-Hägerdal, B., Gorwa-Grauslund, M.F., 2005. Investigation of limiting metabolic steps in the utilization of xylose by recombinant *Saccharomyces cerevisiae* using metabolic engineering. Yeast 22, 359–368.

Kuyper, M., Harhangi, H.R., Stave, A.K., Winkler, A.A., Jetten, M.S., de Laat, W.T., den Ridder, J.J., Op den Camp, H.J., van Dijken, J.P., Pronk, J.T., 2003. High-level functional expression of a fungal xylose isomerase: the key to efficient ethanolic fermentation of xylose by *Saccharomyces cerevisiae*? FEMS Yeast Res. 4, 69–78.

Kuyper, M., Hartog, M.M., Toirkens, M.J., Almering, M.J., Winkler, A.A., van Dijken, J.P., Pronk, J.T., 2005. Metabolic engineering of a xylose-isomerase-expressing *Saccharomyces cerevisiae* strain for rapid anaerobic xylose fermentation. FEMS Yeast Res. 5, 399–409.

Kuyper, M., Winkler, A.A., van Dijken, J.P., Pronk, J.T., 2004. Minimal metabolic engineering of *Saccharomyces cerevisiae* for efficient anaerobic xylose fermentation: a proof of principle. FEMS Yeast Res. 4, 655–664.

Lee, T.H., Kim, M.D., Park, Y.C., Bae, S.M., Ryu, Y.W., Seo, J.H., 2003. Effects of xylulokinase activity on ethanol production from D-xylulose by recombinant *Saccharomyces cerevisiae*. J. Appl. Microbiol. 95, 847–852.

Madhavan, A., Tamalampudi, S., Srivastava, A., Fukuda, H., Bisaria, V.S., Kondo, A., 2009. Alcoholic fermentation of xylose and mixed sugars using recombinant *Saccharomyces cerevisiae* engineered for xylose utilization. Appl. Microbiol. Biotechnol. 82, 1037–1047.

Madhavan, A., Tamalampudi, S., Ushida, K., Kanai, D., Katahira, S., Srivastava, A., Fukuda, H., Bisaria, V.S., Kondo, A., 2008. Xylose isomerase from polycentric fungus *Orpinomyces*: gene sequencing, cloning, and expression in *Saccharomyces cerevisiae* for bioconversion of xylose to ethanol. Appl. Microbiol. Biotechnol. 82, 1067–1078.

Matsushika, A., Watanabe, S., Kodaki, T., Makino, K., Inoue, H., Murakami, K., Takimura, O., Sawayama, S., 2008. Expression of protein engineered $NADP^+$-dependent xylitol dehydrogenase increases ethanol production from xylose in recombinant *Saccharomyces cerevisiae*. Appl. Microbiol. Biotechnol. 81, 243–255.

Moes, C.J., Pretorius, I.S., vanZyl, W.H., 1996. Cloning and expression of the *Clostridium thermosulfurogenes* D-xylose isomerase gene (xylA) in *Saccharomyces cerevisiae*. Biotechnol. Lett. 18, 269–274.

Mumberg, D., Müller, R., Funk, M., 1995. Yeast vectors for the controlled expression of heterologous proteins in different genetic backgrounds. Gene 156, 119–122.

Petschacher, B., Nidetzky, B., 2008. Altering the coenzyme preference of xylose reductase to favor utilization of NADH enhances ethanol yield from xylose in a metabolically engineered strain of *Saccharomyces cerevisiae*. Microb. Cell Fact 7, 9.

Pitkanen, J.P., Aristidou, A., Salusjarvi, L., Ruohonen, L., Penttila, M., 2003. Metabolic flux analysis of xylose metabolism in recombinant *Saccharomyces cerevisiae* using continuous culture. Metabolic Eng. 5, 16–31.

Richard, P., Toivari, M.H., Penttila, M., 2000. The role of xylulokinase in *Saccharomyces cerevisiae* xylulose catabolism. FEMS Microbiol. Lett. 190, 39–43.

Rizzi, M., Erlemann, P., Buithanh, N.A., Dellweg, H., 1988. Xylose Fermentation by Yeasts .4. Purification and Kinetic-Studies of Xylose Reductase from *Pichia-Stipitis*. Appl. Microbiol. Biotechnol. 29, 148–154.

Rudolf, A., Karhumaa, K., Hahn-Hägerdal, B., 2009. Ethanol production from traditional and emerging raw materials. In: Satyanarayana, T., Kunze, G. (Eds.), Yeast Biotechnology: Diversity and Applications. Springer, Netherlands.

Runquist, D., Fonseca, C., Rådström, P., Spencer-Martins, I., Hahn-Hägerdal, B., 2009. Expression of the Gxf1 transporter from *Candida intermedia* improves fermentation performance in recombinant xylose-utilizing *Saccharomyces cerevisiae*. Appl. Microbiol. Biotechnol. 82, 123–130.

Runquist, D., Hahn-Hägerdal, B., Bettiga, M., 2010a. Increased ethanol productivity in xylose-utilizing *Saccharomyces cerevisiae* via a randomly mutagenized xylose reductase. Appl. Environ. Microbiol. 76, 7796–7802.

Runquist, D., Hahn-Hägerdal, B., Rådström, P., 2010b. Comparison of heterologous xylose transporters in recombinant *Saccharomyces cerevisiae*. Biotechnol. Biofuels 3, 5.

Sambrook, J., Fritch, E., Maniatis, T., 1989. Molecular Cloning: A Laboratory Manual, 2nd ed. Cold Spring harbor Laboratory Press, Cold Spring Harbor, New York.

Sarthy, A.V., McConaughy, B.L., Lobo, Z., Sundstrom, J.A., Furlong, C.E., Hall, B.D., 1987. Expression of the *Escherichia coli* xylose isomerase gene in *Saccharomyces cerevisiae*. Appl. Environ. Microbiol. 53, 1996–2000.

Satrustegui, J., Bautista, J., Machado, A., 1983. NADPH/$NADP^+$ ratio: regulatory implications in yeast glyoxylic acid cycle. Mol. Cell Biochem. 51, 123–127.

Schmidt, H., Jirstrand, M., 2006. Systems biology toolbox for MATLAB: a computational platform for research in systems biology. Bioinformatics 22, 514–515.

Sonderegger, M., Jeppsson, M., Hahn-Hägerdal, B., Sauer, U., 2004. Molecular basis for anaerobic growth of *Saccharomyces cerevisiae* on xylose, investigated by global gene expression and metabolic flux analysis. Appl. Environ. Microbiol. 70, 2307–2317.

Teusink, B., Passarge, J., Reijenga, C.A., Esgalhado, E., van der Weijden, C.C., Schepper, M., Walsh, M.C., Bakker, B.M., van Dam, K., Westerhoff, H.V., Snoep, J.L., 2000. Can yeast glycolysis be understood in terms of in vitro kinetics of the constituent enzymes? Testing biochemistry. Eur. J. Biochem. 267, 5313–5329.

Teusink, B., Walsh, M.C., van Dam, K., Westerhoff, H.V., 1998. The danger of metabolic pathways with turbo design. Trends Biochem. Sci. 23, 162–169.

Tewari, Y.B., Steckler, D.K., Goldberg, R.N., 1985. Thermodynamics of the Conversion of Aqueous Xylose to Xylulose. Biophys. Chem. 22, 181–185.

Tochampa, W., Sirisansaneeyakul, S., Vanichsriratana, W., Srinophakun, P., Bakker, H.H.C., Chisti, Y., 2005. A model of xylitol production by the yeast *Candida mogii*. Bioproc. Biosys. Eng. 28, 175–183.

Träff, K.L., Jönsson, L.J., Hahn-Hägerdal, B., 2002. Putative xylose and arabinose reductases in *Saccharomyces cerevisiae*. Yeast 19, 1233–1241.

Träff, K.L., Otero Cordero, R.R., van Zyl, W.H., Hahn-Hägerdal, B., 2001. Deletion of the GRE3 aldose reductase gene and its influence on xylose metabolism in recombinant strains of *Saccharomyces cerevisiae* expressing the xylA and XKS1 genes. Appl. Environ. Microbiol. 67, 5668–5674.

van Maris, A.J., Winkler, A.A., Kuyper, M., de Laat, W.T., van Dijken, J.P., Pronk, J.T., 2007. Development of efficient xylose fermentation in *Saccharomyces cerevisiae*: xylose isomerase as a key component. Adv Biochem. Eng. Biotechnol. 108, 179–204.

Van Vleet, J.H., Jeffries, T.W., Olsson, L., 2008. Deleting the para-nitrophenyl phosphatase (pNPPase), PHO13, in recombinant *Saccharomyces cerevisiae* improves growth and ethanol production on D-xylose. Metabolic Eng. 10, 360–369.

Vanbastelaere, P., Vangrysperre, W., Kerstershilderson, H., 1991. Kinetic-studies of Mg^{2+}-activated, Co^{2+}-activated and Mn^{2+}-activated D-xylose isomerases. Biochem. J. 278, 285–292.

Van Dijken, J.P., Scheffers, W.A., 1986. Redox balances in the metabolism of sugars by yeasts. Fems Microbiol. Rev. 32, 199–224.

Wahlbom, C.F., Eliasson, A., Hahn-Hägerdal, B., 2001. Intracellular fluxes in a recombinant xylose-utilizing *Saccharomyces cerevisiae* cultivated anaerobically at different dilution rates and feed concentrations. Biotechnol. Bioeng. 72, 289–296.

Walfridsson, M., Bao, X., Anderlund, M., Lilius, G., Bülow, L., Hahn-Hägerdal, B., 1996. Ethanolic fermentation of xylose with *Saccharomyces cerevisiae* harboring the *Thermus thermophilus* xylA gene, which expresses an active xylose (glucose) isomerase. Appl. Environ. Microbiol. 62, 4648–4651.

Watanabe, S., Abu Saleh, A., Pack, S.P., Annaluru, N., Kodaki, T., Makino, K., 2007. Ethanol production from xylose by recombinant *Saccharomyces cerevisiae* expressing protein-engineered NADH-preferring xylose reductase from *Pichia stipitis*. Microbiology 153, 3044–3054.

Wisselink, H.W., Cipollina, C., Oud, B., Crimi, B., Heijnen, J.J., Pronk, J.T., van Maris, A.J., 2010. Metabolome, transcriptome and metabolic flux analysis of arabinose fermentation by engineered Saccharomyces cerevisiae. Metab. Eng. 12, 537–551.

Zeng, Q.K., Du, H.L., Wang, J.F., Wei, D.Q., Wang, X.N., Li, Y.X., Lin, Y., 2009. Reversal of coenzyme specificity and improvement of catalytic efficiency of *Pichia stipitis* xylose reductase by rational site-directed mutagenesis. Biotechnol. Lett. 31 (7), 1025–1029.